Numerical Study of the Effects of Residual Stress in Welded Tube Joints

Gustavo T. Silva[1], Lucas P. Gouveia[1], Eduardo T. L. Junior[1], João P. L. Santos[1]

[1]*Laboratory of Scientific Computing and Visualization, Federal University of Alagoas*
Av. Lourival Melo Mota, Tabuleiro do Martins, 57072-970, Maceió - AL, Brazil
gustavo.silva@lccv.ufal.br, lucasgouveia@lccv.ufal.br, limajunior@lccv.ufal.br, jpls@lccv.ufal.br

Abstract. Studies related to the distributions and levels of residual stress arising from the thermal cycles involved in welding processes are of vital importance for evaluating and guaranteeing the integrity of welded tubes. This work proposes the implementation of a routine in Python language to automate the construction of thermomechanical coupling welding models using the ABAQUS® CAE finite element tool, considering the heat distribution model of the welding source as the double ellipsoid model. The studies are produced considering an ambient temperature of 20°C and another with preheating of the tubes to 300°C. The results achieved by this study are related solely to a thin-walled tube joint manufactured in AISI 304 stainless steel, welded using TIG (Tungsten Inert Gas) processes in a single pass. Thus, this study aims to analyze the distributions of residual hoop stresses within post-welded tube in the weld bead and transverse directions in the angular positions 0°, 90°, 180° and 270°, with or without uniform preheating of the pre-welded tube. The results show that, in general, residual stresses differ slightly along the weld beads, as well as with the angular position, being relatively high when compared to the yield stress of the steel, and, therefore, have a considerable impact on the reduction of the mechanical resistance of the welded joint. It is also worth noting that when considering the preheating of the tube, there is an increase in the peak temperature reached in the transfer process, and a decrease in the cooling rate and residual stress levels of the joints, especially in the most critical regions, located in the center of the weld beads.

Keywords: TIG welding process, Goldak model, Preheating, Residual stress.

1 Introduction

In summary, welding is a fundamental process for joining metallic materials, with diverse applications in different industrial sectors. Choosing the appropriate welding process depends on several factors, and knowledge of the techniques and materials used is essential to guarantee the quality of the joints. For [1] and [2], although welding offers several advantages, it is important to highlight that the thermal cycles inherent to the process can induce microstructural changes, contributing to the development of residual stresses and distortions, compromising, in some cases, the integrity of the joint. The authors [3] emphasize that the accurate characterization of residual stresses in welded structures demands a multidisciplinary approach. While experimental methods provide insights for a specific region, computational analysis allows us to obtain a global view of the stress distribution. The combination of both approaches can provide a complete and reliable assessment. According to [4], the use of the finite element method to predict the levels and distributions of residual stresses in welded parts has become popular, as it allows for a more accurate analysis, reducing the occurrence of defects and the need for post-welding treatments, contributing to improving the structural integrity.

In the view of [5], the heat source distribution and movement model of [6] (double ellipsoid model) is widely adopted in numerical simulations of welding processes, as it allows a more realistic representation of heat sources, contributing to a better understanding of the physical phenomena involved in the melting and solidification between the base material and the addition material. In this context, for [7], the residual stresses are a consequence of the thermal and mechanical history of the material during the welding process. Preheating treatments are used to modify the thermal cycle, adjusting the permanence time at elevated temperatures and cooling rates, aiming to minimizing residual stresses.

2 Thermomechanical Model

In the transient thermal analysis of welding processes, the temperature field T depends directly on the time t, the Cartesian coordinates x, y and z, and the energy balance applied to an infinitesimal control volume, as indicated by Eq. (1). In this equation k_i, ρ, C are, respectively, the thermal conductivity in the x, y or z directions, the density, and the specific heat of the steel as a function of temperature, while $\dot{q}$ refers to the internal heat generation rate. There is also heat exchange by convection and radiation in the welding process, but the thermal conduction, described by Eq. (1), is dominant.

$$\frac{\partial}{\partial x}\left(k_x \cdot \frac{\partial T}{\partial x}\right) + \frac{\partial}{\partial y}\left(k_y \cdot \frac{\partial T}{\partial y}\right) + \frac{\partial}{\partial z}\left(k_z \cdot \frac{\partial}{\partial z}\right) + \dot{q} = \rho \cdot C \cdot \frac{\partial T}{\partial t} \tag{1}$$

In coupled thermomechanical analysis, initially, a thermal analysis is performed to determine the temperature field in the part. Subsequently, these results are used as input data for structural analysis, where the stresses and strains of the mechanical model are calculated considering thermal effects. In structural analysis, temperature distributions, acting as thermal loads, generate residual stresses in the material. This analysis also considers the possibility of developing plastic strains in the material, adopting the von Mises criterion to define the beginning of flow, assuming that the material presents an isotropic hardening [3]. The total stiffness matrix $[D^{\mathrm{ep}}]$ comes from the sum of the elastic $[D^{\mathrm{e}}]$ and plastic $[D^{\mathrm{p}}]$ stiffness matrices, as indicated in Eq. (2).

$$[D^{\mathrm{ep}}] = [D^{\mathrm{e}}] + [D^{\mathrm{p}}] \tag{2}$$

Thus, the constitutive relationship between stresses σ and thermal strain ϵ is given by Eq. (3). In this same equation $\left[C^{\mathrm{th}}\right]$ represents the thermal stiffness matrix.

$$[\mathrm{d}\sigma] = [D^{\mathrm{ep}}]\,[\mathrm{d}\varepsilon] - \left[C^{\mathrm{th}}\right]\mathrm{d}T \tag{3}$$

2.1 Heat Source Model According to Goldack et al (1984)

Three-dimensional modeling of the heat source during welding is crucial for understanding the thermal and metallurgical phenomena involved. The [6] model, based on two overlapping ellipsoids, is widely used for this purpose. The geometric parameters of the model a_r, a_f, b and c are obtained and adjusted for each welding process experimentally and made available in the literature, allowing the temperature distribution and the formation of the weld bead to be accurately predicted. The heat source is modeled as a point concentrated at the origin of the Cartesian system (x ,y ,z), as seen in Fig. 1. The model allows analyzing the thermal distribution resulting from the concentration of energy in this point.

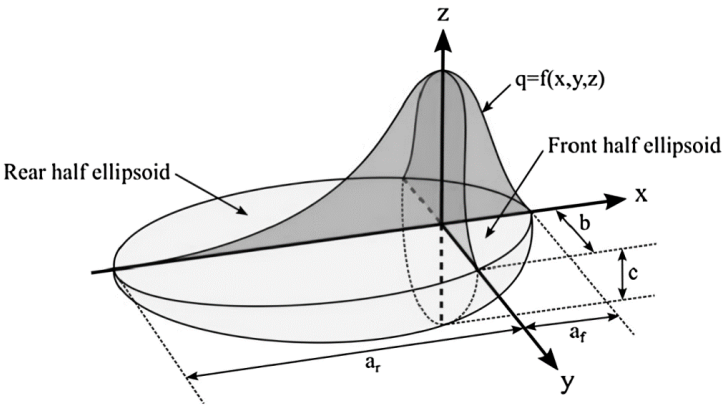

Figure 1. Model of the welding source according to [6].

The distribution of heat flux density $\dot{q}$ during the welding process, according to the model by [6], is defined by two distinct equations: Eq. (4) for the region in front of the weld bead ($x \geq 0$) (front half ellipsoid) and Eq. (5) for the posterior region ($x \leq 0$) (rear half ellipsoid). The parameters η, V and I represent, respectively, the welding efficiency, voltage and amperage of the process.

$$\dot{q}(x,y,z) = \frac{12 \cdot \sqrt{3} \cdot a_f \cdot \eta \cdot V \cdot I}{a_f \cdot (a_f + a_r) \cdot b \cdot c \cdot \pi \cdot \sqrt{\pi}} \cdot e^{-\left(\frac{3 \cdot x^2}{a_f{}^2} + \frac{3 \cdot y^2}{b^2} + \frac{3 \cdot z^2}{c^2}\right)} \tag{4}$$

$$\dot{q}(x,y,z) = \frac{12 \cdot \sqrt{3} \cdot a_r \cdot \eta \cdot V \cdot I}{a_r \cdot (a_f + a_r) \cdot b \cdot c \cdot \pi \cdot \sqrt{\pi}} \cdot e^{-\left(\frac{3 \cdot x^2}{a_r{}^2} + \frac{3 \cdot y^2}{b^2} + \frac{3 \cdot z^2}{c^2}\right)} \tag{5}$$

2.2 Residual Stresses

According to [8], the main problems associated with any fusion welding process are the occurrence of residual stresses and distortions. Residual stresses, a result of the welding thermal cycle, are caused by the plastic yield of the material around the molten zone. Still for [8], the contraction of the metal as it cools generates tensile stresses, mainly in the longitudinal direction of the weld, which can compromise the structural integrity and useful life of the part. The analysis reveals residual stresses of both tensile and compressive character in the transverse and weld bead directions upon cooling. These stresses arise due to the inherent mismatch in thermal contraction between the weld metal and the base material.

3 Methodology

3.1 Model Generation

The generation of models for welding simulation begins with the automation of their creation, using the Python language routine executed by the ABAQUS® CAE software. This routine's main function is to automate the construction of numerical models and the insertion of initial and boundary conditions appropriate to the welding processes in question, in addition to enabling post-processing of numerical results. The models address a thin-walled tube with a thickness of 1.5875 mm, a external diameter of 203.2 mm and a length of 304.8 mm, while the weld bead it has a width of approximately 1.8334 mm.

3.2 Temperature-Dependent Properties of Steel

This study uses AISI 304 stainless steel with some of its temperature-dependent thermal and mechanical properties according to [9] to generate its results. These properties are specific heat, thermal conductivity, coefficient of thermal expansion, density, Young's modulus, Poisson's ratio, and yield and tensile stress, considering a bilinear elastoplastic constitutive model.

3.3 Type of Welding Process and its Specifications

TIG (Tungsten Inert Gas) welding process, considered in this study, is widely used in several industrial sectors and according to [10], it stands out for the high precision and quality of the weld beads. This feature makes it ideal for applications that require a high level of reliability and safety, such as in the oil and gas, aerospace and nuclear industries. This study considers that the mentioned process has a welding efficiency of 0.6, as the production of weld beads is done in a single pass. As for the geometric parameters of the weld point, associated with the [6] model and indicated in Fig. 1, their values are a_r = 6.8, a_f = 1.7, b = 4 and c = 4, both in mm, and are indicated in the work of [11]. The welding parameters such as electrical voltage and amperage of the source are equal to 23 V and 150 A. In the same way, the welding speed of the process is approximately 6.667 mm/s.

3.4 Initial and Boundary Conditions

In this study, the initial condition is represented by the initial temperature of the tube before welding. In other words, the tubes must be at an ambient temperature of 20°C or at a preheating temperature of 300°C. Thermal boundary conditions are divided into heat transfer processes between the tubes and the environment, covering convection and radiation, and internal heat generation produced by the welding source and attributed to each finite element that makes up the weld bead. Convection and radiation heat exchange conditions are applied throughout the body of the tube, whose convection coefficient and emissivity are 15 W/m²°C and 0.6, respectively. When it comes to the mechanical boundary condition, encastres are applied to the ends of the tube. It should be emphasized that in this modeling there are no finite elements birth throughout the process (the additive process is disregarded), only the representation of the movement of the welding source due to the internal energy generation (body heat flux) of each element that represents the weld bead.

3.5 Mesh and Finite Elements

The finite element mesh produced for the tube models has 180 and 87 divisions in the hoop and axial directions, respectively, while it has only one element in its thickness, this is because this represents a single welding pass. The finite element used in the analyzes is the C3D8T (8-node trilinear displacement and temperature). According [12], the ABAQUS® CAE C3D8T element is an eight-node trilinear volumetric element with thermal capacity. This means it allows you to model deformation and heat transfer in three-dimensional materials. This element is used in stationary and transient thermomechanical simulations, as in this modeling.

4 Results and Discussions

The results of this study seek, essentially, to analyze the distributions of residual hoop stresses in the walls of post-welded tubes in the weld bead directions and angular positions 0°, 90°, 180° and 270°, whether or not there is uniform preheating of the tubes before welding. However, the results of the differences presented in the temperature fields and thermal cycles of the processes with and without preheating must also be presented, as a way of contextualizing the development of residual stresses in the welded tubes.

4.1 Temperature Fields

The analysis of the graphical results presented in Fig. 2 (a) e (b) indicates that there are small discrepancies in the temperature profiles between the tubes. However, the tube subjected to preheating stands out for presenting a slightly higher peak nodal temperature at the welding point, reaching a value of 2,216.96°C, approximately 1.435% superior to the tube without preheating, which developed a peak value of 2,185.15°C.

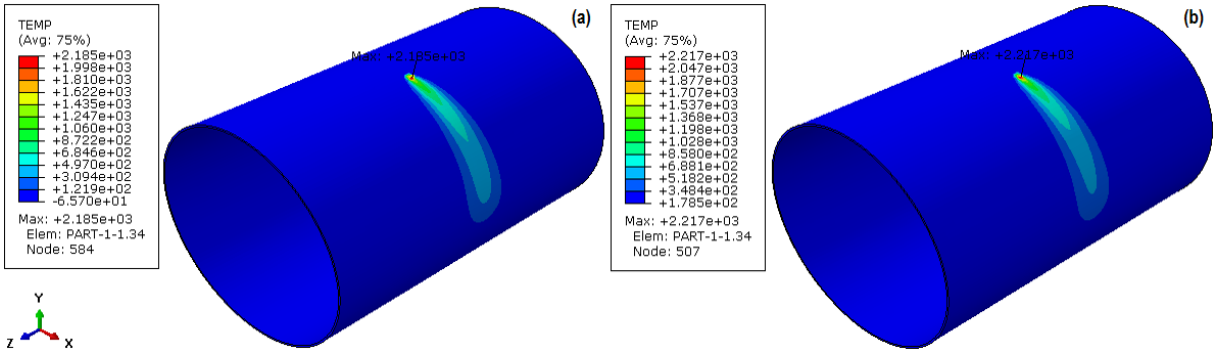

Figure 2. Temperature fields without preheating (a) and with preheating (b).

It is important to highlight that a cooling step of the weld bead is also considered in this modeling, observed by the development of isotherms around the welding point, as seen in Fig. 2 (a) e (b).

4.2 Thermal Cycles

The welding thermal cycles for the two cases present some differences, among them are the peak temperature, as mentioned in the section 4.1 section, and the cooling rates of the weld beads, as shown in Fig. 3.

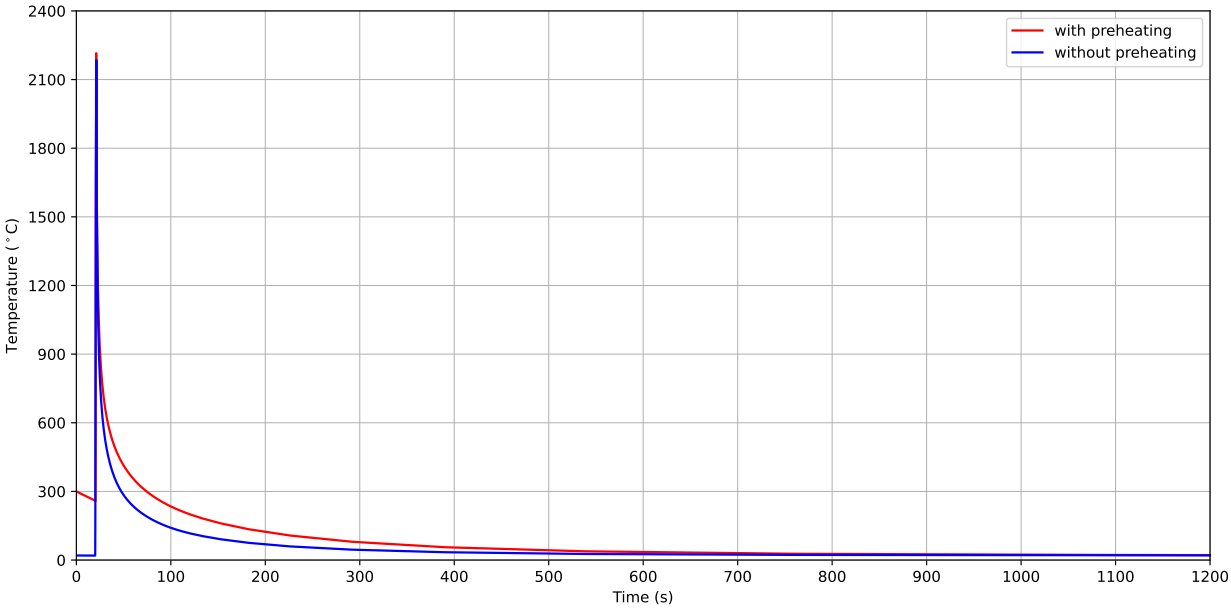

Figure 3. Thermal cycles without and with preheating at one point of the weld.

As for the cooling rates of the weld beads for both cases, these are calculated in the time interval between the peak temperature and the time of 100 s. Under these conditions, the tube without preheating has a cooling rate of approximately 25.87°C/s, while the preheated tube has this same rate in the order of 25.04°C/s. These results indicate that preheating offers a decrease in the cooling rate of the weld beads, while it should have a positive impact on the reduction of residual stresses, as presented in the next section.

4.3 Residual Stresses

In this section, residual hoop stresses are evaluated in the weld bead and transverse directions. The residual stress fields can be observed in Fig. 4 (a) and (b) without and with preheating of the tubes, respectively. In general, it is observed that the greatest residual hoop stresses are developed along the central region of the weld beads for the process without preheating, reaching a value of 303.09 MPa. For the tube with preheating, the maximum residual stress value reaches 231.15 MPa.

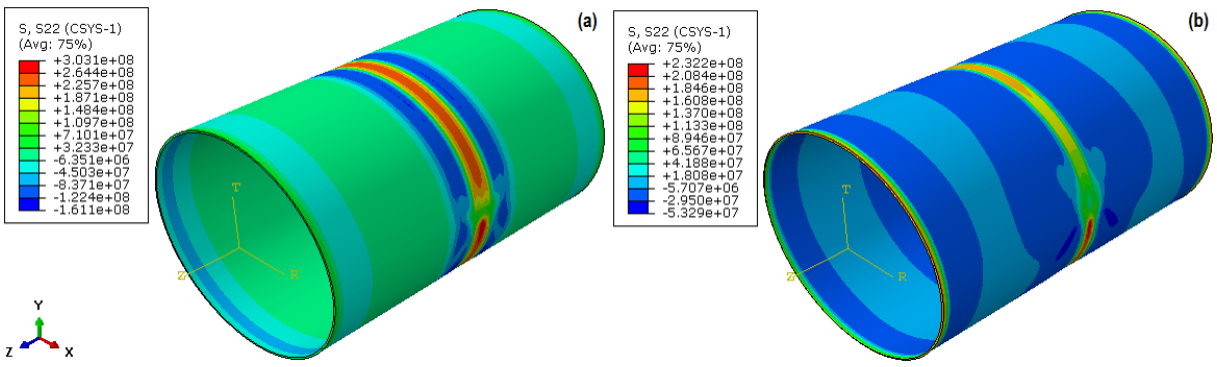

Figure 4. Residual hoop stress field for tubes without preheating (a) and with preheating (b).

The Fig. 5 shows the distribution of residual hoop stresses along the center of the weld beads, without and with preheating, respectively, It should be noted that the angular positions start in the direction of the positive x-axis and increase counterclockwise around the z-axis for the cylindrical coordinate system considered in the modeling. Note that in fact the consideration of tube preheating causes the maximum residual hoop stresses along the weld bead to be lower. From the Fig. 5 it can be observed that the maximum stresses develop in angular positions close to the end of the pass, while the minimum stresses develop at initial angles.

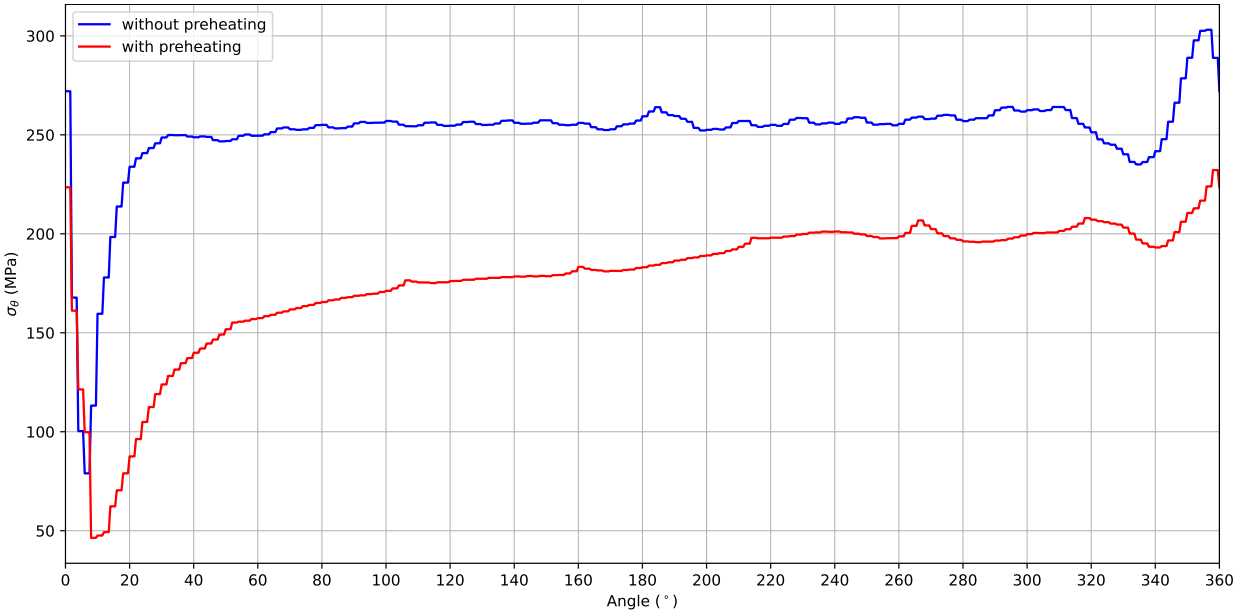

Figure 5. Residual hoop stress distributions along the weld beads.

The residual hoop stress profiles along the direction transverse to the weld bead for the angular positions of 0°, 90°, 180° and 270°, without and with the presence of preheating, they can be observed in Fig. 6. These results indicate that the highest tensile residual stresses occur at the center of the weld bead, especially the welding point located at 0° for the tube without preheating.

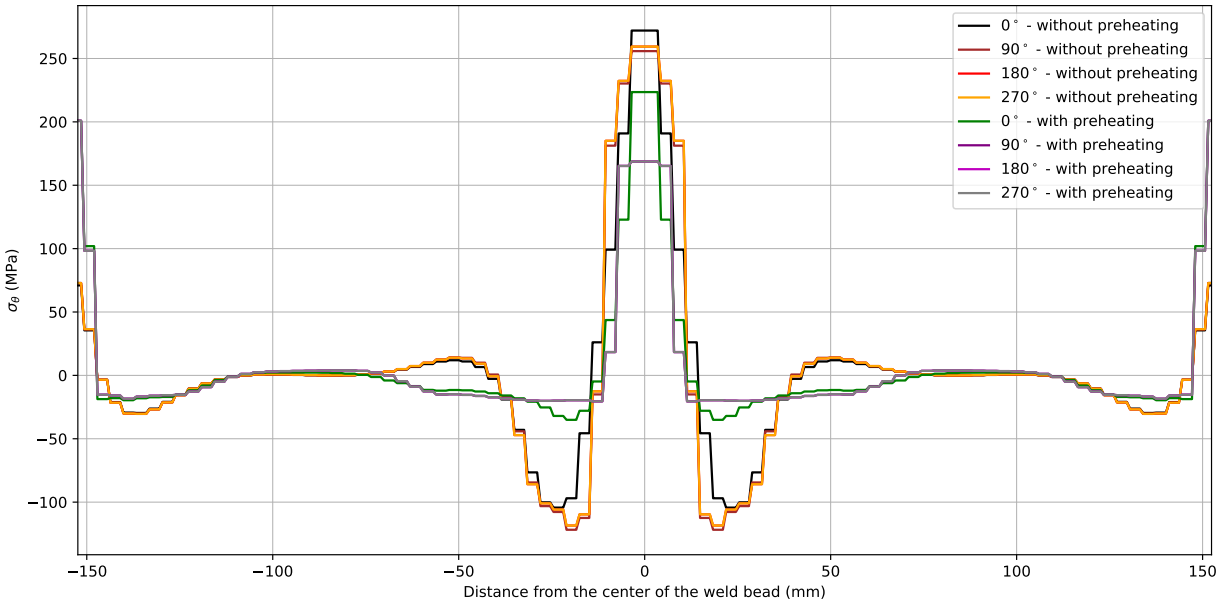

Figure 6. Residual hoop stress profiles along the transverse direction as a function of angle.

Likewise, compressive stresses are more pronounced for the tubes without preheating, as seen at the points with angles of 90° and 270°. Note also that preheating induced a significant decrease in compressive stresses around the weld bead.

5 Conclusions

Preheating is an important tool for controlling residual stresses in welding and improving the quality and durability of weld beads and welded joints. By reducing thermal gradients, increasing ductility and promoting a more homogeneous distribution of stresses, preheating contributes to the manufacture of safer and more reliable parts and structures.

The research findings indicate that preheating tubes prior to welding effectively diminishes, and in certain cases substantially reduces, both tensile and compressive residual hoop stresses. This reduction is particularly pronounced in regions adjacent to and central to the weld bead, resulting in improved performance in a variety of manufacturing applications.

By preheating the tubes, a controlled slowdown in the cooling rate of the weld bead is achieved. This deliberate reduction in the formation of the temperature gradient mitigates, often significantly, the development of residual stresses within the weld, leading to the structural integrity of the joint.

The stress analysis conducted in this study reveals that the largest tensile residual stress magnitudes are concentrated in the core of the weld bead. These peak stresses are notably more severe at the 0° weld point in tube that have not undergone preheating.

The analysis reveals that tubes without preheating exhibit a steeper compressive residual stress field, characterized by peaks at 90° and 270° to the weld bead. Implementing preheating results in a more uniformly distributed stress profile and a substantial reduction in the maximum compressive stresses around the weld.

Acknowledgements. The first author is grateful for the scholarship granted by the Alagoas State Research Support Foundation, Brazil - FAPEAL.

Authorship statement. The authors hereby confirm that they are the sole liable persons responsible for the authorship of this work, and that all material that has been herein included as part of the present paper is either the property (and authorship) of the authors, or has the permission of the owners to be included here.

References

[1] E. S. V. Marques, F. J. G. Silva, and A. B. Pereira. Comparison of finite element methods in fusion welding processes: a review. *Metals*, 2020.

[2] R. Beygi, E. Marques, and L. Silva. Thermomechanical analysis in welding, 2022.

[3] R. Sepe, E. Armentani, and R. Esposito. The influence of thermal properties and preheating on residual stresses in welding. *International Journal of Computational Materials Science and Surface Engineering*, 2007.

[4] P. Knoedel, S. Gkatzogiannis, and T. Ummenhofer. Practical aspects of welding residual stress simulation. *Journal of Constructional Steel Research*, 2017.

[5] N. Moslemi, S. Gohari, B. Abdi, I. Sudin, H. Ghandvar, N. Redzuan, S. Hassan, A. Ayob, and S. Rhee. A novel systematic numerical approach on determination of heat source parameters in welding process. *Journal of Materials Research and Technology*, 2022.

[6] J. A. Goldak, A. P. Chakravarti, and M. Bibby. A new finite element model for welding heat sources. *Metallurgical Transactions*, 1984.

[7] T. L. Teng and C. C. Lin. Effect of welding conditions on residual stresses due to butt welds. *International Journal of Pressure Vessels and Piping*, 1998.

[8] P. Colegrove, C. Ikeagu, A. Thistlethwaite, S. Williams, T. Nagy, W. Suder, A. Steuwer, and T. Pirling. Welding process impact on residual stress and distortion. *Science and technology of welding and joining*, 2009.

[9] D. Deng and H. Murakawa. Numerical simulation of temperature field and residual stress in multi-pass welds in stainless steel pipe and comparison with experimental measurements. *Computational Materials Science*, 2006.

[10] N. Jeyaprakash, A. Haile, and M. Arunprasath. The parameters and equipments used in TIG welding: a review. *The International Journal of Engineering and Science*, 2015.

[11] F. Guangming, M. I. L. Souza, and S. Estefen. Transient temperature distribution analysis using Goldak's double ellipsoidal moving heat source. *Brazilian Congress of Research and Development in Oil and Gas*, 2011.

[12] Hibbitt, Karlsson, and Sorensen. ABAQUS/CAE user's manual, 2002.